Monitoring Endoplasmic Reticulum-to-Golgi Traffic of a Plant Calreticulin by Protein Glycosylation Analysis†

Lorella Navazio,‡ Manuela Miuzzo,‡ Louise Royle,§ Barbara Baldan,‡ Serena Varotto,|| Anthony H. Merry,§ David J. Harvey,§ Raymond A. Dwek,§ Pauline M. Rudd,*,§ and Paola Mariani‡

Dipartimento di Biologia, Università di Padova, Via U. Bassi 58/B, 35131 Padova, Italy, Glycobiology Institute, Department of Biochemistry, University of Oxford, South Parks Road, Oxford OX1 3QU, United Kingdom, and Dipartimento di Agronomia Ambientale e Produzioni Vegetali, Università di Padova, Via Romea 16, 35020 Legnaro (Padova), Italy

Received July 11, 2002; Revised Manuscript Received September 30, 2002

ABSTRACT: Calreticulin is a ubiquitous and highly conserved Ca^{2+}-binding protein that is involved in intracellular Ca^{2+} homeostasis and molecular chaperoning in the endoplasmic reticulum (ER). Plant calreticulin, in contrast to its animal counterpart, is often glycosylated: its *N*-glycans have been shown so far to be of the high-mannose type, typical of ER-resident glycoproteins. During the characterization of calreticulin from vegetative and reproductive tissues of *Liriodendron tulipifera* L., we gained some biochemical evidence that prompted us to investigate the monosaccharide composition and primary structure of the calreticulin *N*-glycans isolated from the ovary of this dicotyledon tree. The structures of the components of the *N*-glycan pool were elucidated by HPLC analysis and exoglycosidase sequencing, and further confirmed by matrix-assisted laser desorption/ionization mass spectrometry. The 16 identified oligosaccharide structures, which consisted of both the high-mannose and complex type, are indicative of calreticulin glycan processing through the ER-to-Golgi pathway up to the medial and trans Golgi stacks. Approximately 45% of calreticulin glycan chains are of the complex type, always containing β(1,2)-xylose, and approximately a third of these also contain α(1,3)-fucose in the core. The most complex glycoform harbors the Lewis-a epitope Galβ1−3[Fucα1−4]GlcNAc. Immunolocalization of calreticulin with anti-calreticulin antibodies was consistent with protein transit through the Golgi. Thus, although it contains the tetrapeptide HDEL ER retention signal, the reticuloplasmin calreticulin possesses the competence to transit from the ER compartment to the distal Golgi stacks. The final fate of the protein after its complete maturation is still obscure.

Most biologically active proteins are known to be glycosylated. Glycosylation strongly affects the physicochemical features and biological functions of proteins. The N-glycosylation cell machinery adds and gradually reshapes oligosaccharide chains attached to specific sites that are encoded in the amino acid sequence of the protein (*1*).

The modifications of the glycan portion of glycoproteins occurring in the endoplasmic reticulum (ER)[1] give rise to only limited diversity, since the same oligosaccharide structures are found on very different proteins. Compared to the uniformity of glycans originating in the ER, a wider structural diversity is introduced in glycoproteins during the transport through the Golgi, resulting in a high heterogeneity of glycosylated variants. This structural diversification potentially leads to the acquisition of novel functions for the glycans displayed in the fully mature proteins. Proteins which reside in the compartments of the secretory pathway are themselves frequently glycosylated, and their oligosaccharide composition provides evidence of their location (*2*).

The ubiquitous Ca^{2+}-binding reticuloplasmin calreticulin, which has been implicated in many cellular functions (*3*), possesses, in its amino acid sequence, potential *N*-glycosylation site(s). In animal calreticulins, the most conserved consensus site for *N*-glycosylation is residue 326 (*4*). Additional consensus sequences for glycosylation are present at position 162 for bovine brain (*5*) and *Schistosoma mansoni* (*6*) calreticulin, and at positions 126 and 154 of the *Leishmania donovani* protein (*7*). Only calreticulin from bovine liver and brain (*5*, *8*), rat liver (*9*), and Chinese hamster ovary cells (*10*) has actually been found to be glycosylated. Glycan structural analysis provided evidence for post-ER glycan maturation on calreticulin from bovine brain (*5*) and rat liver (*9*), suggesting that the protein passes through the Golgi before being recycled back to the ER. To

† This work was supported by the Ministero Università Ricerca Scientifica e Tecnologica (to P.M.).

* To whom correspondence should be addressed. Telephone: +44 1865 275340. Fax: +44 1865 275796. E-mail: pmr@glycob.ox.ac.uk.

‡ Dipartimento di Biologia, Università di Padova.

§ Glycobiology Institute, Department of Biochemistry, University of Oxford.

|| Dipartimento di Agronomia Ambientale e Produzioni Vegetali, Università di Padova.

[1] Abbreviations: ABS, *A. ureafaciens* sialidase; AMF, almond meal fucosidase; 2-AB, 2-aminobenzamide; BSA, bovine serum albumin; BTG, bovine testes β-galactosidase; Con A, concanavalin A; DEAE, diethylaminoethyl; DHB, dihydroxybenzoic acid; DIG, digoxygenin; EC, European Commission; endo H, endoglycosidase H; ER, endoplasmic reticulum; Fuc, fucose; Gal, galactose; Glc, glucose; GlcNAc, *N*-acetylglucosamine; GU, glucose units; HPLC, high-performance liquid chromatography; JBH, Jack bean β-*N*-acetylhexosaminidase; JBM, Jack bean α-mannosidase; Le^a, Lewis-a; MALDI, matrix-assisted laser desorption/ionization; Man, mannose; MS, mass spectrometry; NP, normal-phase; PAGE, polyacrylamide gel electrophoresis; PBS, phosphate-buffered saline; PNGase, peptide *N*-glycosidase; RT, room temperature; SDS, sodium dodecyl sulfate; SPG, *St. pneumoniae* galactosidase; TOF, time-of-flight; Xyl, xylose.

10.1021/bi0204701 CCC: $22.00
Published on Web 11/08/2002

date, glycosylation of calreticulin seems to be species- and/or tissue-specific (*4*).

In plant calreticulins, the potential glycosylation site at Asn326 that is found in animal calreticulins is not conserved, and a putative *N*-glycosylation consensus sequence is preferentially located at position 32 in the *N*-domain. Additional glycosylation sites are present in some species, either in the same region or in the C-domain (*11*). These glycosylation site(s) have been shown to be occupied by glycan(s) in several plant species. Concanavalin A (Con A) binding (*12*−*15*) and more detailed structural analyses (*16*, *17*) support the assignment of a high-mannose structure for the glycan moiety of plant calreticulin. Although this type of glycan is consistent with the ER localization of the protein, experiments with brefeldin A indicate that plant calreticulin is competent for *N*-glycan maturation when the *N*-glycans meet the Golgi enzyme pool (*17*, *18*). Furthermore, Crofts et al. (*18*) demonstrated that, in tobacco cells, calreticulin deprived of the ER retention signal HDEL is secreted and during the transport through the Golgi acquires *N*-glycan modifications carried out by the activity of glycan-processing enzymes that reside therein. The same processing occurs in cells overproducing calreticulin where the retention mechanism is saturated and small amounts of the protein are secreted. The secreted form is endoglycosidase H (endo H)-resistant, which demonstrates that glycan modifications have occurred during the transit through the Golgi (*18*).

In a search for calreticulin from different structures of the dicotyledon tree *Liriodendron tulipifera* L., in leaves and pollen, two bands of 56 and 54 kDa were found to strongly cross-react with antibodies against spinach calreticulin. In the ovary, i.e., the fertile part of the female reproductive organ of the plant, only one major protein band of 56 kDa with the same biochemical features was apparent. In all the samples that were investigated, the calreticulin protein band of 56 kDa was found to bind the lectin Con A on blotting (L. Navazio et al., unpublished results). In this paper, we have characterized, in further detail, calreticulin from the ovary and analyzed the structure of its *N*-glycans. We report that this naturally occurring reticuloplasmin bears, in addition to high-mannose glycan chains, complex-type oligosaccharides, indicative of glycoprotein processing and maturation inside the Golgi apparatus and rather atypical for a classical ER-resident glycoprotein.

EXPERIMENTAL PROCEDURES

Plant Material. Flowers were collected from *L. tulipifera* L. trees, grown in the Botanical Garden of Padova (Padova, Italy). Pollinated ovaries (∼1 kg) were frozen in liquid N_2 and stored at −80 °C until they were used.

Protein Extraction. Protein crude extracts were prepared by grinding *L. tulipifera* ovaries to a fine powder under liquid nitrogen and resuspending them in protein extraction buffer [0.1 M Tris-HCl (pH 7.8), 0.2 M NaCl, 0.2% Triton X-100, 1 mM EDTA, 0.5 mM phenylmethanesulfonyl fluoride, and 1 μM leupeptin] using 4 mL of buffer for each gram of tissue. The homogenates were centrifuged at 20000*g* for 10 min at 4 °C, and the supernatant was collected for SDS−PAGE analysis.

Isolation of calreticulin from *L. tulipifera* ovaries was carried out using a selective ammonium sulfate precipitation procedure, followed by DEAE-cellulose (Whatman, Maidstone, U.K.) column chromatography, as described previously (*19*). All operations were carried out at 4 °C. DEAE-cellulose fractions collected between 0.2 and 0.4 M NaCl were pooled and subjected to concanavalin A (Con A)−Sepharose (Sigma, St. Louis, MO) column chromatography, as previously described for the purification of calreticulin from spinach leaves (*14*). Protein concentrations were determined using the protein assay reagent (Bio-Rad, München, Germany), which is based on the Bradford method (*20*), using bovine serum albumin (BSA) as the standard. *N*-Terminal amino acid sequencing of the 56 kDa protein from the SDS−PAGE gel band was carried out on an Applied Biosystems (Perkin-Elmer, Foster City, CA) 476A protein sequencer, as described previously (*21*).

SDS−PAGE and Western Blotting Techniques. One-dimensional SDS−PAGE was carried out according to the method of Laemmli (*22*) on 7.5 to 10% linear gradient gels. Two-dimensional electrophoresis was performed according to the method described by O'Farrell (*23*) with isoelectric focusing in the first dimension (pH gradient from 4 to 6.5). Peptide mapping after partial digestion with *Staphylococcus aureus* V8 protease (Sigma) of the protein bands excised from preparative SDS−PAGE was carried out according to the method described in ref *24*.

Gels were stained first with Coomassie blue (Sigma) and then with "Stains-All" (Bio-Rad) as described previously (*25*). Proteins separated by SDS−PAGE and transferred electrophoretically onto nitrocellulose membranes (*26*) were analyzed with different types of ligand overlay. $^{45}Ca^{2+}$ overlay was carried out as described previously (*27*). Overlay with horseradish peroxidase-conjugated Con A was performed as previously described (*14*). For immunoblotting analysis, blots were incubated with anti-spinach calreticulin antibodies [1:2000 dilution (*14*)] and the monoclonal antibody 2E7 against the ER retention signal HDEL [1:200 dilution, (*28*)].

Release of N-Linked Glycans. Individual protein bands were excised from Coomassie blue-stained SDS−PAGE gels. In situ deglycosylation with PNGase F (Roche, Mannheim, Germany) was carried out as described in ref *29*.

For deglycosylation with PNGase A, peptides were released from protein gel bands by overnight incubation at 37 °C with 12.5 μg/mL trypsin [1:10 (w/w) enzyme:substrate ratio] in 25 mM ammonium bicarbonate. The supernatant was dried, resuspended in H_2O, heated at 100 °C for 10 min to inactivate the trypsin, and dried again. Liberation of *N*-glycans was carried out by overnight incubation at 37 °C of the tryptic peptide mixture with 18 milliunits/mL PNGase A (Calbiochem, La Jolla, CA) in 100 mM citrate/phosphate buffer (pH 5.0) (personal communication from D. A. Ashford, York, U.K.). Sugars were purified from protein and salts by passing the sugars through Millipore $ZipTip_{C18}$ filtration devices followed by AG3X4(OH^-) (bottom)/AG50X12(H^+) (middle)/C18 (top) mixed bed resins.

Fluorescent Labeling with 2-Aminobenzamide. The glycan pool was evaporated to dryness using a vacuum centrifuge and fluorescently labeled via a reductive amination reaction with 2-AB using the Oxford Glycoscience's Signal Labelling Kit (*30*), and excess reagent was removed by ascending paper chromatography with acetonitrile.

Simultaneous Exoglycosidase Sequencing of the Released Glycan Pool. Aliquots of the PNGase A-released *N*-glycans were evaporated to dryness in a vacuum centrifuge. The 2-AB-labeled oligosaccharides were digested in a volume of 10 μL for 18 h at 37 °C in 50 mM sodium acetate buffer (pH 5.5) using arrays of the following enzymes: 1 unit/mL *Arthrobacter ureafaciens* sialidase (ABS, EC 3.2.1.18), 3 milliunits/mL almond meal α-fucosidase (AMF, EC 3.2.1.111), 0.1 unit/mL *Streptococcus pneumoniae* galactosidase (SPG, EC 3.2.1.23), 1 unit/mL bovine testes β-galactosidase (BTG, EC 3.2.1.23), 10 milliunits/mL Jack bean β-*N*-acetylhexosaminidase (JBH, EC 3.2.1.30), and 50 units/mL Jack bean α-mannosidase (JBM, EC 3.2.1.24) (for incubations with Jack bean α-mannosidase, the enzyme was added, the mixture incubated overnight, then a second aliquot added, and the mixture incubated for a further 8 h). All enzymes were purchased from Glyko, Inc. (Novato, CA). After incubation, enzymes were removed by filtration through a protein binding nitrocellulose membrane (Pro-Spin 45 μm CN filters, Radley and Co., Ltd., Essex, U.K.), and oligosaccharides were analyzed by NP-HPLC.

Analysis of N-Glycans by Normal Phase High-Performance Liquid Chromatography (NP-HPLC). NP-HPLC separations were performed using a TSK-Gel Amide-80 4.6 mm × 250 mm column (Tosoh Biosep LLC) fitted to a Water Alliance 2690 Separations module equipped with a Jasco FP-920 fluorescence detector (E_{ex} = 330 nm, E_{em} = 420 nm). Solvent A was 50 mM formic acid adjusted to pH 4.4 with an ammonia solution. Solvent B was acetonitrile. The column temperature was set to 30 °C. Gradient conditions were a linear gradient from 20 to 58% A, over 152 min at a flow rate of 0.4 mL/min. Samples were injected in 80% acetonitrile. The system was calibrated using an external standard of hydrolyzed and 2-AB-labeled glucose oligomers to create a dextran ladder, as described previously (*31*).

Glycan analyses were carried out on protein preparations from three subsequent blooming seasons, with identical results.

MALDI-TOF MS. Positive ion MALDI-TOF mass spectra were recorded with a Micromass TofSpec 2E reflectron-TOF mass spectrometer [Micromass (UK) Ltd., Wythenshawe, Manchester, U.K.] fitted with delayed extraction and a nitrogen laser (337 nm). The acceleration voltage was 20 kV; the pulse voltage was 3200 V, and the delay for the delayed extraction ion source was 500 ns. Samples were prepared by adding 0.5 μL of an aqueous solution of the sample to the matrix solution [0.3 μL of a saturated solution of 2,5-dihydroxybenzoic acid (DHB) in acetonitrile] on the stainless steel target plate and allowing it to dry at room temperature (RT). The sample/matrix mixture was then recrystallized from ethanol (*32*).

Immunocytochemistry. Specimens from *L. tulipifera* ovaries were fixed for 24 h at 4 °C in 4% (v/v) formaldehyde and 0.25% (v/v) glutaraldehyde in 0.1 M phosphate buffer (pH 7.2); samples were subsequently dehydrated in an ethanol series and embedded in medium-grade LR White acrylic resin (TAAB, Aldermaston Berks, U.K.). Ultrathin sections collected on Ni grids were labeled on-drop. Briefly, nonspecific protein binding sites were saturated in 3% BSA in phosphate-buffered saline (PBS) for 1 h at RT. Grids were incubated with anti-spinach calreticulin antibodies, diluted (1:100) in PBS, for 2 h at RT, rinsed twice in PBS, incubated with gold-conjugated goat anti-rabbit antibody (GAR 15; BioCell, Cardiff, U.K.), diluted 1:30 in PBS, for 1 h at RT, and washed three time in PBS and once in distilled H_2O. Grids were exposed to OsO_4 vapors overnight, counterstained with uranyl acetate, and observed under a Hitachi 300 electron microscope operating at 75 kV.

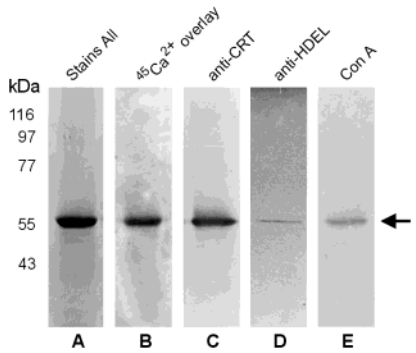

FIGURE 1: Biochemical characterization of calreticulin from *L. tulipifera* ovary. Protein fractions which eluted between 0.2 and 0.4 M NaCl from a DEAE-cellulose column were analyzed by Stains-All staining of SDS−PAGE (A), $^{45}Ca^{2+}$−ligand overlay of blot (B), immunoblot with anti-calreticulin antibodies (C), immunoblot with anti-HDEL antibodies (D), and affinoblot with Con A (E). The arrow indicates calreticulin (CRT).

In Situ Hybridization. Ovaries were dissected and fixed in 4% paraformaldheyde in 0.1 M phosphate buffer at 4 °C overnight and embedded in Paraplast Plus (Sigma). Sections of ~7 μm were obtained using a microtome (Leica, Heerbrugg, Switzerland). Before hybridization, paraffin was removed and the slides were pretreated with 5 μg/mL proteinase K and hybridized with sense and antisense digoxygenin (DIG)-UTP-labeled RNA probes obtained by in vitro transcription with T3 and T7 transcriptases following the manufacturer's instructions (Roche). A maize calreticulin 1.6 kb cDNA clone (*13*) was used as template to transcribe the probes. Hybridization was carried out in 50% formamide at 42 °C for 16 h. After hybridization, slides were extensively washed with 2× SSC buffer at 45 °C and treated with 20 μg/mL RNAase A. Detection and visualization of the signal on the tissues were carried out by reaction with an alkaline phosphatase anti-DIG-conjugated antibody and a color assay using as substrates nitroblue tetrazolium and 5-bromo-4-chloro-3-indolyl phosphate following the manufacturer's instructions (Roche). Images were acquired by using dedicated ImageNT software connected to a Leica DMR microscope.

RESULTS

Identification and Purification of Calreticulin from the Ovary of L. tulipifera L. Calreticulin was isolated from the ovary of *L. tulipifera* by an ammonium sulfate precipitation procedure followed by anion exchange chromatography on DEAE-cellulose. The identity of the protein as calreticulin was verified by Stains-All staining of SDS−PAGE, by $^{45}Ca^{2+}$ overlay on-blot, and by immunodetection with anti-calreticulin antibodies (Figure 1). The 56 kDa calreticulin was found to cross-react with antibodies against the ER retention signal HDEL and to label with Con A (Figure 1).

The spatial distribution of calreticulin mRNA was assessed by in situ hybridization on ovary sections. The signal was

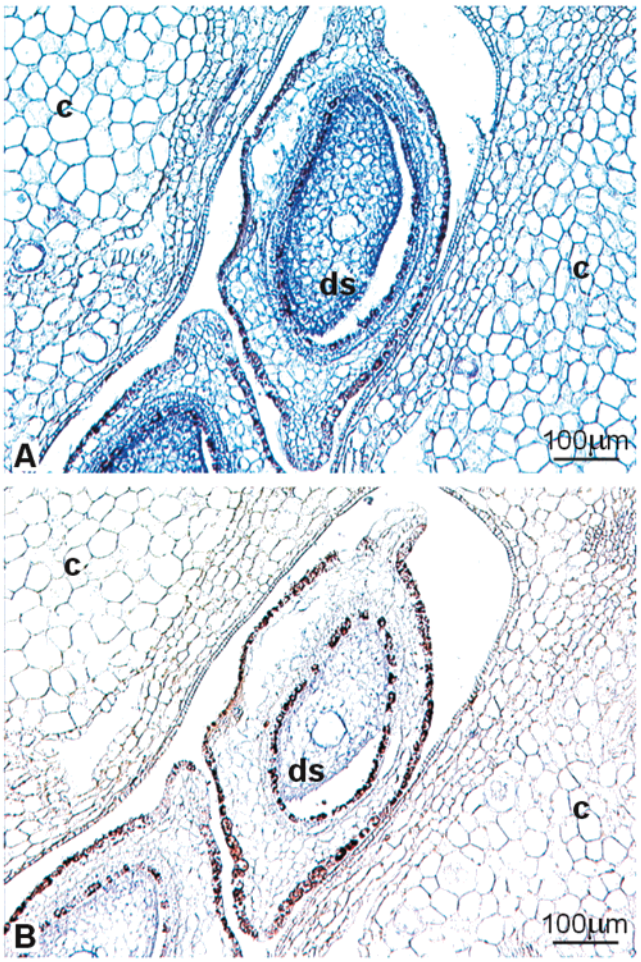

FIGURE 2: Localization of CRT mRNA in *L. tulipifera* ovary sections. (A) Hybridization pattern with the antisense probe. The labeling is widespread through the entire section, with a stronger signal in developing seeds. (B) Incubation with the sense probe (negative control). The hybridization signal is visualized by the blue staining. c, carpel tissues; ds, developing seeds.

found to be widespread in all ovary tissues, with stronger labeling in developing seeds (Figure 2).

When DEAE-cellulose protein fractions were applied to a Con A−Sepharose column, both the retained fraction and flow-through were found to contain a 56 kDa Stains-All blue staining band (Figure 3A), which exhibited a strong cross-reactivity with anti-calreticulin antibodies (Figure 3B). The possibility that the presence of calreticulin in the flow-through could be due to column overloading was ruled out because the subsequent application of the same sample on a second Con A−Sepharose column resulted in the total recovery of the 56 kDa protein in the new flow-through (data not shown). Con A binding on-blot further confirmed that only the 56 kDa protein recovered in the fraction retained in the Con A−Sepharose column, but not in the flow-through, could be labeled with the lectin (Figure 3C). Both calreticulin proteins were found to share the same *N*-terminal amino acid sequence (DVFFEERFDDGxEN for calreticulin retained by the Con A−Sepharose column and DVFFEERFDD for the protein in the flow-through). Moreover, the two proteins displayed the same isoelectric point (pI 4.7) and a totally superimposable peptide map, obtained by partial digestion with *S. aureus* V8 protease (data not shown). The same apparent molecular masses of the two calreticulin

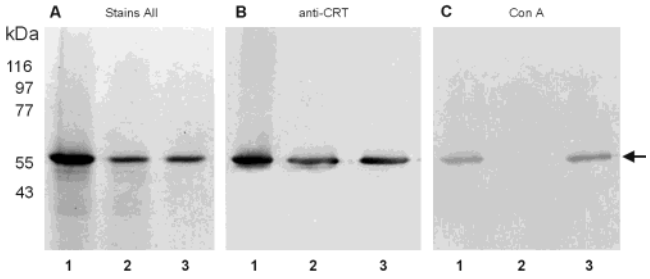

FIGURE 3: Affinity chromatography on a Con A−Sepharose column. DEAE-cellulose fractions from *L. tulipifera* ovary were loaded onto a Con A−Sepharose column, and bound proteins were eluted with 0.2 M methyl α-D-mannopyranoside. Protein samples were resolved by SDS−PAGE, and either stained with Stains-All (A) or transferred to nitrocellulose and incubated with anti-calreticulin antibodies (B) or Con A (C): lane 1, DEAE-cellulose fraction applied to a Con A−Sepharose column; lane 2, flow-through; and lane 3, sample retained and subsequently eluted from the column. The arrow indicates calreticulin (CRT).

proteins may indicate that they represent glycosylated variants (glycoforms) of a single polypeptide.

Analysis of Calreticulin N-Glycans by High-Performance Liquid Chromatography (HPLC) and Matrix-Assisted Laser Desorption/Ionization (MALDI) Time-of-Flight (TOF) Mass Spectrometry (MS). Glycans were released from calreticulin, which was extracted from *L. tulipifera* ovary by DEAE-cellulose chromatography. The protein was run on a SDS−PAGE gel and the 56 kDa band excised for glycan release. Two different endoglycosidases were used to release the *N*-glycans: peptide *N*-glycosidase A (PNGase A), which is able to liberate all *N*-glycans, including those bearing an α-(1,3)fucose residue linked to the proximal GlcNAc of the core; and PNGase F, which releases *N*-glycans which do not contain a core α(1,3)fucose residue (*33*). The released glycans were fluorescently labeled with 2-aminobenzamide (2-AB) and analyzed by NP-HPLC (Figure 4). The top panel of Figure 4 shows the whole *N*-glycan pool released by PNGase A. The middle panel shows the *N*-glycans released by PNGase F and, therefore, do not contain a core α(1,3)-fucose. The bottom panel shows *N*-glycans which were released from calreticulin by PNGase A following PNGase F treatment, and hence, they all contain a core α(1,3)fucose. This figure clearly demonstrates the presence of glycans both with and without a core α(1,3)fucose.

Aliquots of the total PNGase A-released *N*-glycan pool were then digested with a range of exoglycosidases, singly and in arrays. The NP-HPLC analyses of these digests are shown in Figure 5 and Table 1. The whole *N*-glycan pool was also analyzed by MALDI-TOF mass spectrometry, and the results are shown in Figure 6 and Table 1. Structures were assigned on the basis of their NP-HPLC elution positions, measured in glucose units (GU) (*31*) before and after exoglycosidase digestion, and from their masses as obtained from MALDI-TOF mass spectrometry (*34*). Approximately 55% of the total pool consisted of high-mannose glycans [peaks 5, 10, 13, 16, and 17 being $(Man)_{5-9}(GlcNAc)_2$, respectively] that were digested with Jack bean α-mannosidase (JBM). The remaining glycans had paucimannosidic-type or complex structures, all of which contained xylose (determined by mass spectrometry and GU values), and

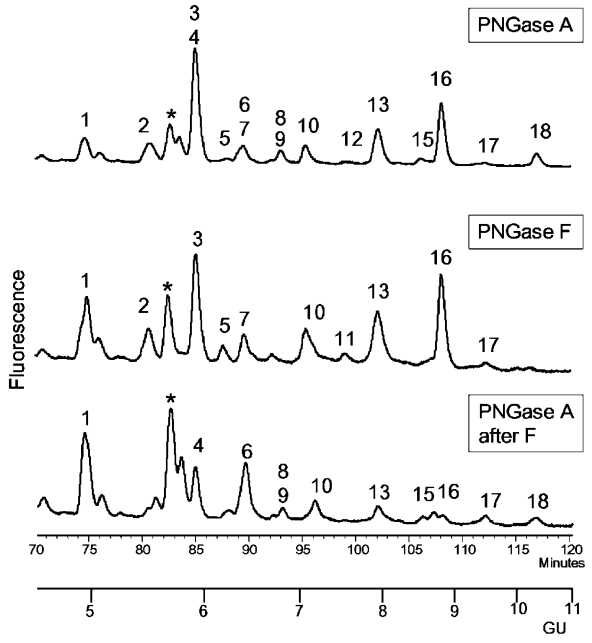

FIGURE 4: NP-HPLC chromatograms of 2-AB-labeled *N*-glycans released enzymatically from calreticulin of *L. tulipifera* ovary: (top) *N*-glycans released by PNGase A from trypsin-digested gel bands, (middle) *N*-glycans released directly from gel bands by PNGase F, and (bottom) after in situ deglycosylation with PNGase F, gel bands were digested with trypsin and remaining *N*-glycans removed with PNGase A (see Experimental Procedures for full details). The glycan structures corresponding to the numbers on the HPLC peaks are listed in Table 1.

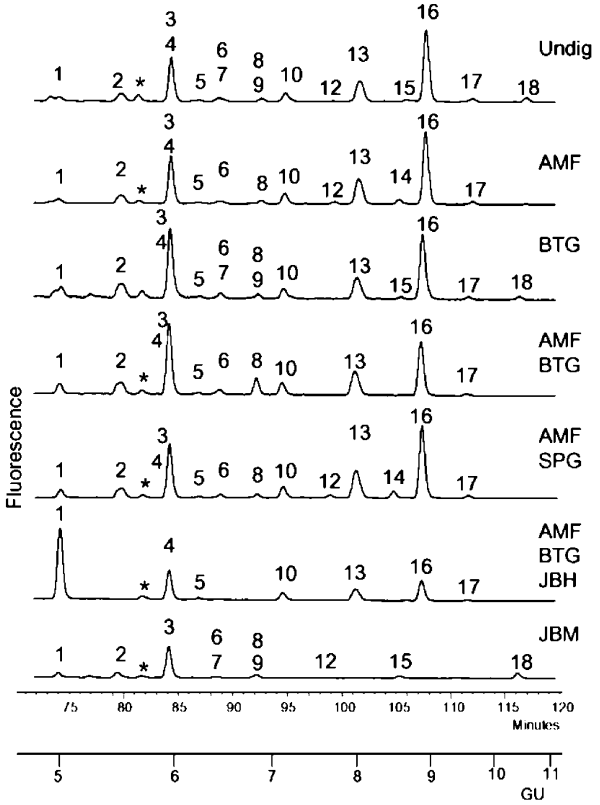

FIGURE 5: Exoglycosidase sequencing of *N*-glycans from *L. tulipifera* ovary calreticulin monitored by NP-HPLC. Aliquots of the total PNGase A-released 2-AB-labeled *N*-glycan pool were incubated with a range of exoglycosidases, as shown in each panel. The percent areas and structures of the different glycans detected by this method are listed in Table 1. Exoglycosidases: AMF, almond meal fucosidase; BTG, bovine testes β-galactosidase; SPG, *St. pneumoniae* galactosidase; JBH, Jack bean β-*N*-acetylhexosaminidase; JBM, Jack bean α-mannosidase.

approximately a third of these also contained a core α(1,3) fucose (ascertained from the different specificities of PNGase A and F). Fucose was also found on the antennae of some glycans as evidenced by its susceptibility to almond meal fucosidase (AMF). This enzyme is unable to digest the core fucose. The α1−4 linkage of the antennary fucose was assigned following the observation that all galactose residues were removed by bovine testes β-galactosidase (BTG), whereas none were removed by the β1−4-specific galactosidase from *St. pneumoniae* (SPG), indicating that all galactose residues were in a β1−3 linkage to GlcNAc. Among the largest peaks were the high-mannose glycans $(Man)_6(GlcNAc)_2$, $(Man)_7(GlcNAc)_2$, and $(Man)_8(GlcNAc)_2$ (10, 13, and 16, respectively). The largest complex glycan that was found (peak 18) was a biantennary carbohydrate containing two Lewis-a (Le^a) structures (Galβ1−3[Fucα1−4]GlcNAc), as well as core α(1,3)fucose and xylose. The abundant peak (3, 4) at GU 5.9 had two different components. The major component (14.8% of the pool) was Compound 3 (Table 1) which is a biantennary ungalactosylated structure which is released by PNGase F and could be digested by Jack bean β-*N*-acetylhexosaminidase (JBH). The second component was Compound 4 (∼5.8% of the pool) which has a $(Man)_3(GlcNAc)_2$ core structure substituted with xylose and α(1,3)fucose, and was only released by PNGase A.

The results of the glycan analysis indicate that calreticulin isolated from the ovary of *L. tulipifera* is a pool of glycosylated variants. This pool was found to contain a range of high-mannose glycans, which are the result of the action of enzymes localized in the ER [$(Man)_{8-9}(GlcNAc_2)$] but also representative of subsequent processing in the Golgi [$(Man)_{5-7}(GlcNAc_2)$]. Furthermore, more than one mature glycoform bearing complex glycan chains was identified. These glycans contained either one or two terminal epitopes containing α(1,4)fucose and β(1,3)galactose residues linked to the GlcNAc units (Table 1, peaks 15 and 18), accounting for ∼3.8% of the total glycan pool. The entire *N*-glycan pool from calreticulin was found to contain at least 16 different structures, many of which may stem from biosynthetic intermediates leading to the fully mature biantennary Le^a-containing structures described above. Notably, all the identified complex glycans contain β(1,2)xylose linked to the β-mannose residue of the core. Approximately one-third also contain α(1,3)fucose linked to the proximal GlcNAc residue of the core. The relative amount of the complex glycans (fully processed structures and intermediary products) was ∼45% of the total calreticulin glycan pool, and the remainder was high-mannose structures.

Immunolocalization of Calreticulin in the Ovary Cells. Electron microscopy using the immuno-gold technique with polyclonal antibodies against spinach calreticulin was applied in examining the intracellular distribution of the protein. The specificity of the anti-calreticulin antibodies was verified by immunoblotting analysis with protein crude extracts from *L. tulipifera* ovary (Figure 7A).

Preferential strong labeling of the Golgi stacks was observed in all ovary cells, irrespective of any cell special-

Table 1: Mass Spectrometric and Exoglycosidase Digestion Data with Sugar Composition and Structures for Glycans Released by PNGase A

Mass [M+Na]$^+$		Composition [a]				GU	Enzymes used [b]							Structure [c]	HPLC Peak No.
							Undig	AMF	BTG	AMF BTG	AMF SPG	AMF BTG JBH	JBM		
Found	Calc.	Hex	HexNAc	Fuc	Xyl										
nd	1185.5	3	2	0	1	**4.90**	4.8	3.0	6.9	4.6	3.3	44.7	2.6		**1**
1388.4	1388.5	3	3	0	1	**5.50**	5.4	5.7	8.5	8.0	6.5	0.0	2.9	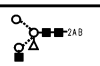	**2**
						5.64	3.6	1.6	3.3	2.2	1.6	2.9	1.0	Gel	*
1591.6	1591.6	3	4	0	1	**5.9**	20.6	21.8	27.4	29.6	22.4	-	14.8	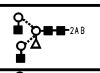	**3**
1331.4	1331.5	3	2	1	1							19.5	-	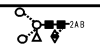	**4**
1377.4	1377.5	5	2	0	0	**6.17**	1.0	1.2	1.0	1.3	1.1	1.4	0.0	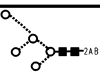	**5**
1534.5	1534.6	3	3	1	1	**6.39**	2.7	2.1	2.5	2.8	1.8	0.6	0.8		**6**
								-		-	-	-		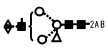	**7**
1737.7	1737.6	3	4	1	1	**6.85**	1.7	2.2	1.8	7.2	2.2	0.0	1.8		**8**
1680.5	1680.6	3	3	2	1									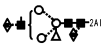	**9**
1539.5	1539.6	6	2	0	0	**7.10**	5.0	5.5	4.9	5.7	5.4	5.2	0.0	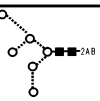	**10**
nd	1915.7	5	4	0	1	**7.30**	0.0	0.3	0.0	0.0	0.5	0.0	0.0	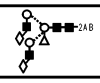 [d]	**11**
nd	1899.7	4	4	1	1	**7.65**	0.4	1.2	0.0	0.0	1.8	0.0	0.6		**12**
1701.6	1701.6	7	2	0	0	**7.90**	14.1	16.2	12.0	14.0	16.7	10.7	0.0	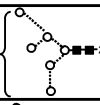	**13**
nd	2061.8	5	4	1	1	**8.50**	0.0	2.9	0.0	0.0	3.2	0.0	0.0	 [d]	**14**
2045.8	2045.8	4	4	2	1	**8.60**	1.5	0.0	1.1	0.0	0.0	0.0	1.5	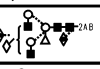	**15**
1863.7	1863.7	8	2	0	0	**8.90**	34.6	34.2	26.7	23.8	32.1	14.0	0.0	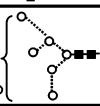	**16**
2025.8	2025.7	9	2	0	0	**9.50**	2.1	1.5	1.5	0.9	1.4	1.1	0.5	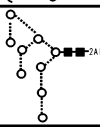	**17**
2353.9	2353.9	5	4	3	1	**10.46**	2.3	0.4	0.0	0.0	0.0	0.0	2.7		**18**

[a] All 2-AB-labeled. Hex, hexose; HexNAc, *N*-acetylhexoseamine; Fuc, fucose; Xyl, xylose. [b] Numbers are percentage areas. [c] The symbols for the glycan structures are as follows: GlcNAc, black square; mannose, white circle; galactose, white diamond; fucose, diamond with a dot inside; xylose, white triangle; β-linkage, solid line; α-linkage, dotted line; -, 1−4 linkage; /, 1−3 linkage; |, 1−2 linkage. [d] Digestion product only. Undig, undigested whole glycan pool. nd, not detected.

ization (Figure 7B). All Golgi cisternae appeared to be specifically labeled, with a more evident concentration of gold particles at the trans side (Figure 7B, top panel). Some vesicles appeared to also be marked close to the ER (Figure 7B, bottom panel) and the Golgi apparatus or, rather rarely, to the plasma membrane. The ER label was poor, probably due to the dilution of the protein inside this large compartment (Figure 7B, bottom panel). This specific labeling demonstrates that calreticulin can move from the ER to the Golgi, where the glycan chains are processed and mature.

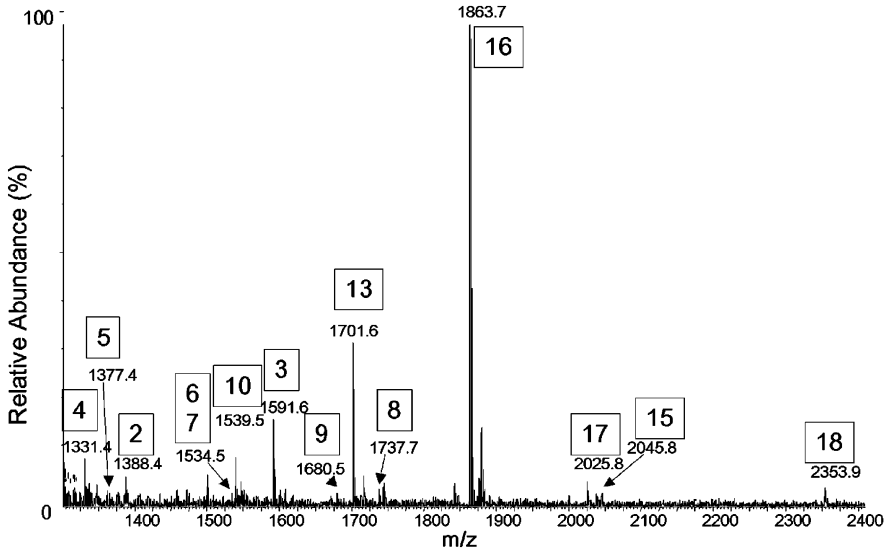

FIGURE 6: MALDI mass spectrum of the 2-AB-labeled *N*-glycan pool released from calreticulin by PNGase A. Numbers in boxes refer to the HPLC peak numbers in Table 1. The composition and structures to the masses shown are also listed in Table 1.

DISCUSSION

In this paper, we provide evidence for the presence in *L. tulipifera* ovary of multiple glycoforms of calreticulin containing both high-mannose and complex-type *N*-glycans.

Glycoproteins with high-mannose glycan chains [$(Man)_{5-9}(GlcNAc)_2$ (*35*)] originate from the activity of specific enzymes that modify the precursor oligosaccharide $(Glc)_3(Man)_9(GlcNAc)_2$ initially attached to Asn residues in the ER. Most ER-resident glycoproteins, including calreticulin, have this type of *N*-linked glycan. Oligomannose-type *N*-glycans have been previously identified as the only oligosaccharides in calreticulin from spinach (*16*) and maize (*17*).

Complex glycans are derived from the processing of oligomannose oligosaccharides by specific glycosidases and glycosyltransferases operating in an ordered sequence in the Golgi apparatus (*36*). In plant cells, the carbohydrate chains of the complex type have a core structure characterized by α(1,3)fucose and/or β(1,2)xylose residues attached to the core proximal GlcNAc and β-mannose residue, respectively. According to ref *37*, fucosylation probably occurs after xylosylation, mainly in the trans Golgi stacks. Further processing involves the attachment of β(1,3)galactose and α(1,4)fucose residues to the terminal GlcNAc, thus leading to larger mono- or biantennary complex glycan moieties. The carbohydrate motif Galβ1−3[Fucα1−4]GlcNAc, named the Le^a antigen in the mammalian counterpart (*38*), is also widely distributed in plants and highly expressed on cell surfaces (*39*−*41*).

The analytical techniques used in this study allowed the rapid and sensitive sequencing of the components of the calreticulin *N*-glycan pool extracted from *L. tulipifera* ovary. In comparison with the rather homogeneous composition of the high-mannose oligosaccharide pool previously identified in calreticulin from both spinach [$(Man)_{7-8}(GlcNAc)_2$ (*16*)] and maize [$(Man)_{8-9}(GlcNAc)_2$ (*17*)], greater diversity was observed in *L. tulipifera* ovary. Indeed, in addition to $(Man)_8(GlcNAc)_2$ (34%), $(Man)_7(GlcNAc)_2$ (14%), $(Man)_6(GlcNAc)_2$ (5%), and $(Man)_5(GlcNAc)_2$ (1%), complex structures (45%) were also identified, indicative of further processing. A critical evaluation of all the identified complex-type struc-

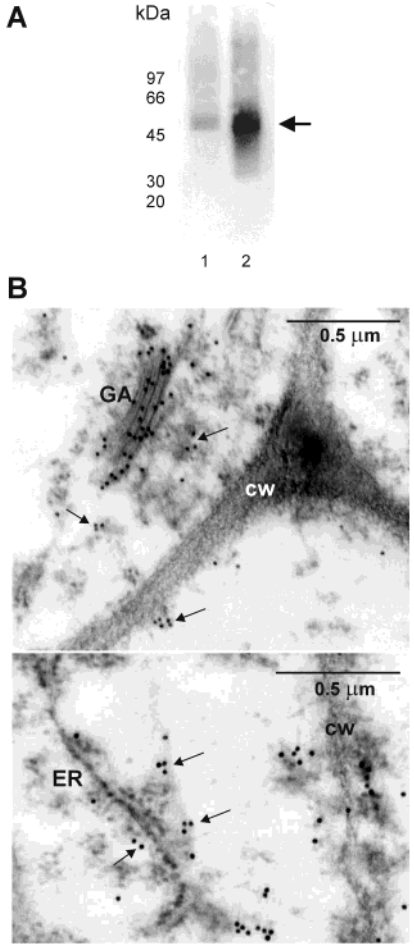

FIGURE 7: Western analysis and immuno-gold labeling of calreticulin in *L. tulipifera* ovary. (A) Total ovary protein extracts (lane 1, 30 μg) were immunostained with anti-spinach calreticulin antibodies after electrophoretic transfer. Purified spinach calreticulin (lane 2, 2 μg) was used as a positive control. The arrow indicates calreticulin. (B, top) Golgi stacks are markedly labeled, mainly at the trans side. Gold particle patches are evident in vesicles close to the Golgi apparatus and the plasma membrane (arrows). (B, bottom) The ER compartment is poorly labeled; gold particles are concentrated inside several vesicles near the ER strand (arrows). cw, cell wall; ER, endoplasmic reticulum; GA, Golgi apparatus.

tures suggests that two major glycan processing pathways are likely to occur during the cis−trans transport through the Golgi. One of them involves the addition of an α(1,3)-fucose residue in the core, and the other one leads to complex glycans lacking this residue in the core. The presence of β-(1,2)xylose in all the identified structures indicates that a common step in both pathways is the transfer of xylose to the β-mannose of the core. Within the two speculative pathways of glycoprotein maturation, several processing intermediary products mark the steps leading to the most mature identified forms, which harbor one or two Le^a antigen epitopes.

The finding of two paucimannosidic-type glycan structures [$(Man)_3(Xyl)(GlcNAc)_2$ and $(Man)_3(Xyl)(Fuc)(GlcNAc)_2$], typical of vacuolar glycoproteins (*35*) in calreticulin, a protein which is completely absent from the vacuole (*42*), suggests that peripheral GlcNAc residues are removed by hydrolases not exclusively located in the vacuolar compartment, as generally reported (*35*).

Most plant calreticulins contain a single potential N-glycosylation site, but in some species, calreticulin has two (*Prunus armeniaca*, *Ricinus communis*, *Beta vulgaris*, and *Nicotiana tabacum*) or three (*Arabidopsis thaliana*) sites. Since calreticulin from *L. tulipifera* has not yet been cloned, it cannot be determined if the heterogeneous population of glycans occupies single or multiple glycosylation sites on the protein.

The oligosaccharide chains of calreticulin from *L. tulipifera* ovary identified by HPLC and MALDI-MS analyses and the immunolocalization of the protein provide strong evidence for the transport of calreticulin outside the ER compartment up to the medial and trans Golgi cisternae. Although calreticulin is generally believed to be efficiently retained in the ER (*17*) or recycled back from the cis Golgi (*43*), our data support the possibility that, under physiological conditions, this protein can exit from the ER and has the competence to be processed in the medial/trans Golgi. At present, due to the limited amount of data available on the glycan structures of plant calreticulins, we cannot speculate about how widespread this glycan processing (which is rather unusual for an ER-resident protein) is.

The final fate of the protein remains to be determined. It is still unknown if, after the complete maturation of the glycan chains, the protein (a) is transported back into the ER (even the glycoforms of calreticulin from the Con A−Sepharose flow-through were found to have HDEL at their C-terminus, data not shown), (b) remains in the Golgi apparatus, as it may be suggested by the strong labeling of this compartment observed by immunocytochemical analysis (ref *44* and Figure 7B in this paper), or (c) proceeds along the secretory pathway up to the plasma membrane, as ascertained in some animal cell types (*45*, *46*), and/or the cell wall.

In plant cells, it is still controversial whether, under physiological conditions, retrograde transport of proteins can occur from beyond the cis Golgi. Crofts et al. (*18*) demonstrated that in tobacco plants, which overexpressed calreticulin, the protein is rapidly secreted and does not recycle back to the ER once complex glycans have been synthesized in the medial/trans Golgi apparatus.

The presence of complex-type *N*-glycans with one or two Le^a epitopes is considered to be indicative of a cell surface localization of the glycoprotein. The Le^a antigen, which has been well characterized in mammalian cells, has recently been found in a wide range of plant cells (*39*−*41*). Its presence on secreted glycoproteins, either soluble or plasma membrane-attached, has led to the hypothesis that the Le^a structure may be involved in the pathogen-induced stress response or in cell-to-cell recognition processes (*40*). However, our immunocytochemical analysis showed only occasional labeling of the plasma membrane and the cell wall. Le^a-containing oligosaccharides have also been immunocytochemically localized in the Golgi apparatus (*40*).

The glycosylation pattern of calreticulin from *L. tulipifera* ovary appears to be specific for the female reproductive organ. Indeed, calreticulin from pollen of the same species does not show any evidence of complex-type glycans (*15*). Given the high immunogenicity of plant complex *N*-glycans, including the Le^a-containing structures (*35*, *47*), it is possible to speculate that the complex-type carbohydrate chains of calreticulin isolated from the ovary of *L. tulipifera* may contribute to the allergenic potential, in particular, of the seeds. Indeed, our in situ hybridization experiments, although not providing information about a possible differential distribution of the glycoforms bearing complex glycans, seem to support a higher level of expression of calreticulin in the developing seeds.

ACKNOWLEDGMENT

We are grateful to D. A. Ashford (York, U.K.) for helpful advice on PNGase A digestion, P. Dainese (Zurich, Switzerland) for performing the N-terminal amino acid sequence analysis, and E. Damiani (Padova, Italy) for valuable suggestions on protein purification. We also thank J. M. Boyce (Oxford, U.K.) and R. Napier (Warwick, U.K.) for the kind gifts of the calreticulin cDNA clone and anti-HDEL antibody, respectively.

REFERENCES

1. Rudd, P. M., Colominas, C., Royle, L., Murphy, N., Hart, E., Merry, A. H., Hebestreit, H. F., and Dwek, R. A. (2001) *Proteomics 1*, 285−294.
2. Helenius, A., and Aebi, M. (2001) *Science 291*, 2364−2369.
3. Michalak, M., Mariani, P., and Opas, M. (1998) *Biochem. Cell Biol. 76*, 779−785.
4. Baksh, S., and Michalak, M. (1996), in *Calreticulin* (Michalak, M., Ed.) pp 11−30, Springer, New York.
5. Matsuoka, K., Seta, K., Yamakawa, Y., Okuyama, T., Shinoda, T., and Isobe, T. (1994) *Biochem. J. 298*, 435−442.
6. Khalife, J., Trottein, F., Schacht, A. M., Godin, C., Pierce, R., and Capron, A. (1993) *Mol. Biochem. Parasitol. 57*, 193−202.
7. Joshi, M., Pogue, G. P., Duncan, R. C., Lee, N. S., Singh, N. K., Atreya, C. D., Dwyer, D. M., and Nakhasi, H. L. (1996) *Mol. Biochem. Parasitol. 81*, 53−64.
8. Khanna, N. C., Tokuda, M., and Waisman, D. M. (1987) *Biochem. J. 242*, 245−251.
9. van Nguyen, P., Peter, F., and Söling, H.-D. (1989) *J. Biol. Chem. 264*, 17494−17501.
10. Jethmalani, S. M., Henle, K. J., and Kaushal, G. P. (1994) *J. Biol. Chem. 269*, 23603−23609.
11. Mariani, P., Navazio, L., and Zuppini, A. (2002) in *Calreticulin in health and disease* (Michalak, M., and Eggleton, P., Eds.) Landes Bioscience, Georgetown, TX.
12. Denecke, J., Carlsson, L. E., Vidal, S., Höglund, A.-S., Ek, B., van Zeijl, M. J., Sinjorgo, K. M. C., and Palva, E. T. (1995) *Plant Cell 7*, 391−406.
13. Napier, R. M., Trueman, S., Henderson, J., Boyce, J. M., Hawes, C., Fricker, M. D., and Venis, M. A. (1995) *J. Exp. Bot. 46*, 1603−1613.

14. Navazio, L., Baldan, B., Dainese, P., James, P., Damiani, E., Margreth, A., and Mariani, P. (1995) *Plant Physiol. 109*, 983−990.
15. Navazio, L., Sponga, L., Dainese, P., Fitchette-Lainé, A.-C., Faye, L., Baldan, B., and Mariani, P. (1998) *Plant Sci. 131*, 35−42.
16. Navazio, L., Baldan, B., Mariani, P., Gerwig, G. J., and Vliegenthart, J. F. G. (1996) *Glycoconjugate J. 13*, 977−983.
17. Pagny, S., Cabanes-Macheteau, M., Gillikin, J. W., Leborgne-Castel, N., Lerouge, P., Boston, R. S., Faye, L., and Gomord, V. (2000) *Plant Cell 12*, 739−755.
18. Crofts, A. J., Leborgne-Castel, N., Hilmer, S., Robinson, D. G., Phillipson, B., Carlsson, L. E., Ashford, D. A., and Denecke, J. (1999) *Plant Cell 11*, 2233−2247.
19. Milner, R. E., Baksh, S., Shemanko, C., Carpenter, M. R., Smillie, L., Vance, J. E., Opas, M., and Michalak, M. (1991) *J. Biol. Chem. 266*, 7155−7165.
20. Bradford, M. M. (1976) *Anal. Biochem. 72*, 248−254.
21. Nardi, M. C., Giacomelli, E., Dainese, P., Fitchette-Lainé, A.-C., Faye, L., Baldan, B., Navazio, L., and Mariani, P. (1998) *Bot. Acta 111*, 66−70.
22. Laemmli, U. K. (1970) *Nature 227*, 680−685.
23. O'Farrell, P. H. (1975) *J. Biol. Chem. 250*, 4007−4021.
24. Cleveland, D. W., Fisher, S. G., Kirschner, M. W., and Laemmli, U. K. (1977) *J. Biol. Chem. 252*, 1102−1106.
25. Campbell, K. P., MacLennan, D. H., and Jorgensen, A. O. (1983) *J. Biol. Chem. 258*, 11267−11273.
26. Towbin, H., Stahelin, T., and Gordon, J. (1979) *Proc. Natl. Acad. Sci. U.S.A. 76*, 4350−4354.
27. Maruyama, K., Mikaawa, T., and Ebashi, S. (1984) *J. Biochem. 95*, 511−519.
28. Napier, R. M., Fowke, L. C., Hawes, C., Leis, M., and Pelham, H. R. B. (1992) *J. Cell Sci. 102*, 261−271.
29. Küster, B., Wheeler, S. F., Hunter, A. P., Dwek, R. A., and Harvey, D. J. (1997) *Anal. Biochem. 250*, 82−201.
30. Bigge, J. C., Patel, T. P., Bruce, J. A., Goulding, P. N., Charles, S. M., and Parekh, R. B. (1995) *Anal. Biochem. 230*, 229−238.
31. Guile, G. R., Rudd, P. M., Wing, D. R., Prime, S. B., and Dwek, R. A. (1996) *Anal. Biochem. 240*, 210−226.
32. Harvey, D. J. (1993) *Rapid Commun. Mass Spectrom. 7*, 614−619.
33. Tretter, V., Altmann, F., and Marz, L. (1991) *Eur. J. Biochem. 199*, 647−652.
34. Harvey, D. J. (1999) *Mass Spectrom. Rev. 18*, 349−451.
35. Lerouge, P., Cabanes-Macheteau, M., Rayon, C., Fitchette-Lainé, A.-C., Gomord, V., and Faye, L. (1998) *Plant Mol. Biol. 38*, 31−48.
36. Keegstra, K., and Raikhel, N. (2001) *Curr. Opin. Plant Biol. 4*, 219−224.
37. Fitchette-Lainé, A.-C., Gomord, V., Chekkafi, A., and Faye, L. (1994) *Plant J. 5*, 673−682.
38. Henry, S., Oriol, R., and Samuelson, B. (1995) *Vox Sang. 6*, 166−182.
39. Fitchette-Lainé, A.-C., Gomord, V., Cabanes, M., Michalski, J.-C., Saint Macary, M., Foucher, B., Cavelier, B., Hawes, C., Lerouge, P., and Faye, L. (1997) *Plant J. 12*, 1411−1417.
40. Fitchette-Lainé, A.-C., Cabanes-Macheteau, M., Marvin, L., Martin, B., Satiat-Jeunemaitre, B., Gomord, V., Crooks, K., Lerouge, P., Faye, L., and Hawes, C. (1999) *Plant Physiol. 121*, 333−343.
41. Melo, N. S., Nimtz, M., Conradt, H. S., Fevereiro, P. S., and Costa, J. (1997) *FEBS Lett. 415*, 186−191.
42. Opas, M., Tharin, S., Milner, R. F., and Michalak, M. (1996) *Protoplasma 191*, 164−171.
43. Phillipson, B., Pimpl, P., Lamberti Pinto daSilva, L., Crofts, A., Taylor, J. P., Movafeghi, A., Robinson, D. G., and Denecke, J. (2001) *Plant Cell 13*, 2005−2020.
44. Borisjuk, N., Sitailo, L., Adler, K., Malysheva, L., Tewes, A., Borisjuk, L., and Manteuffel, R. (1998) *Planta 206*, 504−514.
45. Cho, J.-H., Homma, K., Kanegasaki, S., and Natori, S. (1999) *Eur. J. Biochem. 266*, 878−885.
46. Goicoechea, S., Orr, A. W., Pallero, M. A., Eggleton, P., and Murphy-Ullrich, J. E. (2000) *J. Biol. Chem. 275*, 36358−36368.
47. Rayon, C., Lerouge, P., and Faye, L. (1998) *J. Exp. Bot. 49*, 1463−1472.

BI0204701